

## Effect of impurities on the dielectric response of the charge-density wave in $K_{0.3}MoO_3$

R. J. Cava, L. F. Schneemeyer, R. M. Fleming, P. B. Littlewood, and E. A. Rietman  
*AT&T Bell Laboratories, Murray Hill, New Jersey 07974*

(Received 17 April 1985)

We present the results of experiments in which the characteristics of the low-frequency relaxation of the charge-density wave (CDW) in  $K_{0.3}MoO_3$  "blue bronze" have been determined in the presence of weakly perturbing (Rb substituted for K) and strongly perturbing (W substituted for Mo) impurities. Both the mean relaxation time and static dielectric constant decrease strongly in the presence of the impurities. The temperature dependence of the CDW characteristics has been studied between approximately 25 and 90 K, and displays both similarities and differences from the results we obtained for the pure blue bronze. We discuss the results within the context of the classical model for CDW transport.

### I. INTRODUCTION

Charge transport by means of a moving charge-density wave (CDW), where the CDW can be depinned from the lattice by the application of small electric fields, has been observed in several materials with anisotropic crystal structures. This type of charge transport has been studied extensively in the "blue bronze"  $K_{0.3}MoO_3$  below the CDW onset temperature at 180 K.<sup>1,2</sup> In earlier publications<sup>3,4</sup> we reported the ac conductivity of pure crystals of  $K_{0.3}MoO_3$  at frequencies between 5 Hz and 13 MHz in the temperature range 60–100 K. The data show dispersion in the ac conductivity, behavior generic to this class of materials, which at low temperatures occurs at lower frequencies than observed earlier in such materials as  $NbSe_3$ .<sup>5</sup> Initial inspection of the conductivity data of the pure bronze crystals revealed general characteristics which were those expected from a phenomenological equation of motion of a pinned CDW with an overdamped response to the ac field.<sup>6</sup> This phenomenological equation treats the CDW as a rigid entity with no internal degrees of freedom. The detailed characteristics of the response, however, indicated the existence of significant internal degrees of freedom for the pinned CDW. The conventional ac-conductivity-analysis formalism could not be used to extract information on the internal degrees of freedom of the CDW from the data. Thus we turned to a semiempirical analysis technique developed extensively to describe dielectric relaxation in polymers and polar molecules.

The dielectric response of a system with a single degree of freedom, for an overdamped (relaxation) response, was first derived by Debye:<sup>7</sup>

$$\epsilon(\omega) = \epsilon_{HF} + (\epsilon_0 - \epsilon_{HF}) / (1 + i\omega\tau_0), \quad (1)$$

where  $\epsilon(\omega)$  is the frequency-dependent dielectric response,  $\tau_0$  is the characteristic relaxation time of the step response function,  $\epsilon_0$  is the static dielectric constant ( $\omega \ll 1/\tau_0$ ), and  $\epsilon_{HF}$  is the high-frequency dielectric constant ( $\omega \gg 1/\tau_0$ ). This description, which is equivalent to an overdamped oscillator formalism,<sup>6</sup> is inadequate to describe the ac response in  $K_{0.3}MoO_3$ . Instead, the data

indicated that there exist internal degrees of freedom of the CDW characterized by a distribution of relaxation times about the mean time  $\tau_0$ . Such distributions have been observed extensively in other systems, and indicate in this case that the CDW is not responding as a rigid body as it relaxes to its equilibrium configuration. Further, the data indicated that the distribution of relaxation times of the CDW was not (logarithmically) symmetric about  $\tau_0$ , eliminating from consideration simple symmetric distributions of relaxation times such as Gaussian or block functions. Asymmetric response about  $\tau_0$  had been observed in polymer systems, and a generalization of the Debye formulation, which allows for an asymmetric distribution of relaxation times associated with a single process, was also found to provide an excellent description of the dielectric response of the CDW in  $K_{0.3}MoO_3$ :<sup>8</sup>

$$\epsilon(\omega) = \epsilon_{HF} + (\epsilon_0 - \epsilon_{HF}) / [1 + (i\omega\tau_0)^{1-\alpha}]^\beta, \quad (2)$$

where the exponents  $\alpha$  and  $\beta$  characterize the width and the skewness of the distribution of times about  $\tau_0$ . With this expression one can describe the conventional single-relaxation-time response ( $\alpha=0, \beta=1$ ), the symmetric distribution of relaxation times about  $\tau_0$  ( $\alpha \neq 0, \beta=1$ ) and a general, asymmetric distribution ( $\alpha \neq 0, \beta \neq 1$ ) of times.

By employing expression (2) we characterized the dynamics of the CDW relaxation in  $K_{0.3}MoO_3$  in detail. Several features of the CDW relaxation were discovered in this study: (a) The mean relaxation times are surprisingly long, between  $4.9 \times 10^{-5}$  and  $2.3 \times 10^{-7}$  sec from 60 to 101 K, and display an exponential dependence on temperature. (b) The static dielectric constant  $\epsilon_0$ , which is on the order  $10^6$ – $10^7$ , was also exponentially dependent on temperature. (c) The shape of distribution of relaxation times about the mean time, for times longer than  $\tau_0$ , is strongly temperature dependent, with an increasing fraction of long-time relaxation occurring as the temperature was decreased.

Recent experiments have shown that addition of impurities to the blue bronze strongly effect various properties of the CDW.<sup>9–11</sup> In this study we investigate the effects of such impurities on the CDW relaxation. Again, we

find Eq. (2) to provide an excellent description of the data. We find the addition of impurities to have dramatic effects on the mean relaxation time  $\tau_0$ , the static dielectric constant  $\epsilon_0$ , and the breadth of the distribution of relaxation times.

An important feature of Eq. (2) is that it leads to a cusp in  $\epsilon(\omega)$  of the form  $\epsilon_0 - (i\omega\tau_0)^{1-\alpha}$  at low frequencies  $\omega\tau_0 \ll 1$ . Such a cusp is predicted by simple classical models<sup>12,13</sup> of a pinned charge-density wave in a random potential, and arises from the presence of marginally stable metastable states in the sample with very long relaxation times. A mean-field solution of the Fukuyama-Lee-Rice model gives a cusp with  $|\omega|$  dependence,<sup>14</sup> and numerical simulations in one dimension give a cusp with  $\alpha$  close to 0.5.<sup>15</sup> There is no general prediction for the behavior in three dimensions, but the earlier experiments<sup>3</sup> were fitted to values of  $\alpha$  in the range 0 to 0.25, with  $\alpha$  increasing as the temperature was lowered.

For  $\omega\tau_0 \gg 1$ , Eq. (2) gives  $\epsilon(\omega) \sim (i\omega\tau_0)^{-(1-\alpha)\beta}$ . On general grounds one expects that at high enough frequencies such that the oscillator strength of the pinned CDW modes is exhausted, one should have  $\epsilon(\omega) \sim (i\omega)^{-1}$ , and hence  $\beta \simeq 1/(1-\alpha)$ . It is significant that we found earlier that the product  $\beta(1-\alpha)$ , while temperature independent, had a value of approximately 0.7, and that the high-frequency dielectric constant  $\epsilon_{\text{HF}} \sim 10^3$ . Both of these facts imply the existence of pinned CDW modes at frequencies greater than 10 MHz. We shall return to this point in more detail in Sec. III and IV.

## II. EXPERIMENTAL

The doped  $\text{K}_{0.3}\text{MoO}_3$  crystals employed were grown electrochemically as described elsewhere.<sup>16</sup> Crystals of four compositions were studied. Samples with rubidium partially substituted for potassium at the compositions  $\text{K}_{0.25}\text{Rb}_{0.05}\text{MoO}_3$  and  $\text{K}_{0.15}\text{Rb}_{0.15}\text{MoO}_3$  were taken as examples of the effects of weakly pinning impurities, and samples with tungsten partially substituted for molybdenum,  $\text{K}_{0.3}\text{Mo}_{0.996}\text{W}_{0.004}\text{O}_3$  and  $\text{K}_{0.3}\text{Mo}_{0.99}\text{W}_{0.01}\text{O}_3$ , were taken as examples of the effects of strongly pinning impurities.<sup>10</sup> The complex admittance of the samples was measured between 5 Hz and 13 MHz by a Hewlett-Packard HP4192A impedance analyzer under computer control. Admittance was sampled at 131 frequencies at 20 points per frequency decade on crystals with a two-probe measurement configuration, with current flowing along the crystallographic  $b$  axis. The ac signal amplitude was 4 mV rms or less, depending on the sample impedance. The measurement circuit was balanced such that stray admittances were insignificant at all frequencies for sample impedances greater than approximately 15  $\Omega$ .

The temperature-dependent measurements of sample admittances were performed in a Displex refrigerator. Complex admittances of various samples were measured between temperatures of 25 to 89K and found to have the same general characteristics. Ultrasonic indium contacts were employed and applied in a nitrogen-rich atmosphere. Analysis of sample response in the complex impedance plane<sup>3</sup> allowed us to determine the quality of the contacts, a critical consideration in two-probe measurements. Sam-

ples selected for final study were screened for negligible contact resistance and capacitive coupling at the contacts. Dimensions and threshold fields at 77 K for the four samples selected for final study are presented in Table I. None of the samples showed "switching" in the  $I$ - $V$  response near threshold. Complex admittances were collected on heating, at temperature intervals of 4 K. Threshold fields for nonlinear conductivity were determined from dc  $I$ - $V$  characteristics in voltage-driven response measurements.

## III. RESULTS

Detailed analysis of the pinned CDW response was made in terms of the complex dielectric constants, determined from the measured quantities by the relations  $\epsilon'(\omega) = \text{Im}\sigma(\omega)/\omega$  and  $\epsilon''(\omega) = [\text{Re}\sigma(\omega) - \sigma_{\text{dc}}]/\omega$ .  $\sigma_{\text{dc}}$  was obtained from measured  $\text{Re}\sigma$  at low frequencies where  $\text{Re}\sigma$  was independent of  $\omega$ . The data [ $\epsilon'(\omega)$  and  $\epsilon''(\omega)$ ] were fitted to Eq. [2] for frequencies where  $\text{Re}\sigma - \sigma_{\text{dc}} > 0$  and for  $\text{Im}\sigma > 0$ . Initial values for the parameters at each temperature were obtained from plots of  $\log_{10}\epsilon'$  and  $\log_{10}\epsilon''$  versus  $\log_{10}\omega$ . Fits to the dielectric constant data were performed by minimization of the average agreement index, as defined in Table II, by variation of the parameters  $\tau_0$ ,  $\epsilon_0$ ,  $\alpha$ ,  $\beta$ , and  $\epsilon_{\text{HF}}$ . For all materials  $\epsilon_{\text{HF}}$  was insignificant ( $< 0.5\%$ ) compared to  $\epsilon_0$  at high temperatures and was therefore excluded from the fits until significant. The values determined for  $\tau_0$ ,  $\epsilon_0$ ,  $\epsilon_{\text{HF}}$ ,  $\alpha$ , and  $\beta$ , along with the agreement index  $R$  and characteristics of the data employed in the fit, are presented in Table II for each compound at each temperature. Estimates of the errors are  $\pm 0.02$  for  $\alpha$ ,  $\pm 0.03$  for  $\beta$ ,  $\pm 2\%$  for  $\epsilon_0$ , and  $\pm 3\%$  for  $\tau_0$ . The average agreement values, which are generally between 1 and 2%, indicate the high degree of accuracy to which the dielectric response of the CDW can be described by the formalism developed to describe other types of dielectric relaxation. Figures 1–4 present representative data sets for each material, with the solid lines representing the calculated dielectric response from Eq. (2).

Inspection of Figs. 1–4 and the data presented in Table II reveal significant similarities and differences among the results for the different samples. First, as observed in the undoped  $\text{K}_{0.3}\text{MoO}_3$ , we find the mean relaxation time  $\tau_0$  to be strongly temperature dependent for all materials. We have found mean relaxation times to vary between  $4.1 \times 10^{-4}$  sec ( $\omega_0/2\pi = 388$  Hz) and  $615 \times 10^{-9}$  sec ( $\omega_0/2\pi = 25.9$  MHz) in the temperature range studied. The results and comparison to our earlier data for un-

TABLE I. Characteristics of samples selected for dielectric response studies.

Composition	Length (cm)	Area (cm <sup>2</sup> )	$E_T$ at 77 K (mV/cm)
$\text{K}_{0.25}\text{Rb}_{0.05}\text{MoO}_3$	0.295	0.000 981	680
$\text{K}_{0.15}\text{Rb}_{0.15}\text{MoO}_3$	0.183	0.000 387	1640
$\text{K}_{0.3}\text{Mo}_{0.996}\text{W}_{0.004}\text{O}_3$	0.165	0.000 310	760
$\text{K}_{0.3}\text{Mo}_{0.99}\text{W}_{0.01}\text{O}_3$	0.234	0.001 42	~1200

TABLE II. Parameters describing the dielectric response of the charge-density wave in doped potassium molybdate blue bronzes, where  $\epsilon(\omega) = \epsilon_\infty + (\epsilon_0 - \epsilon_\infty) / [1 + (i\omega\tau_0)^{1-\alpha}]^\beta$ .

Temperature (K)	$\epsilon_0$	$\epsilon_\infty$	$\alpha$	$\beta$	$\beta(1-\alpha)$	$\tau_0$ (sec)	$\omega_0/2\pi$ (Hz)	Number of Data in fit	Agreement (R, %) <sup>a</sup>	$\sigma_0$ <sup>b</sup>
<b>K<sub>0.25</sub>Rb<sub>0.05</sub>MoO<sub>3</sub></b>										
89	$6.30 \times 10^5$		0.08	0.85	0.78	$8.00 \times 10^{-8}$	$1.99 \times 10^6$	88	1.7	7.21
85	$7.54 \times 10^5$		0.07	0.81	0.75	$1.20 \times 10^{-7}$	$1.33 \times 10^6$	94	1.5	5.62
81	$9.25 \times 10^5$		0.10	0.85	0.77	$1.68 \times 10^{-7}$	$9.47 \times 10^5$	94	1.0	4.25
77	$1.12 \times 10^6$		0.08	0.81	0.75	$2.66 \times 10^{-7}$	$5.98 \times 10^5$	112	0.6	3.17
73	$1.37 \times 10^6$		0.08	0.81	0.75	$4.10 \times 10^{-7}$	$3.88 \times 10^5$	130	0.7	2.33
69	$1.65 \times 10^6$	$6.8 \times 10^3$	0.08	0.85	0.78	$5.78 \times 10^{-7}$	$2.75 \times 10^5$	130	0.9	1.73
65	$2.05 \times 10^6$	$1.1 \times 10^4$	0.10	0.87	0.78	$9.27 \times 10^{-7}$	$1.72 \times 10^5$	142	0.8	1.29
61	$2.76 \times 10^6$	$1.1 \times 10^4$	0.13	0.93	0.81	$1.65 \times 10^{-6}$	$9.65 \times 10^4$	150	1.1	$8.26 \times 10^{-1}$
57	$3.27 \times 10^6$	$1.2 \times 10^4$	0.16	0.98	0.82	$2.66 \times 10^{-6}$	$5.98 \times 10^4$	156	1.2	$5.77 \times 10^{-1}$
53	$3.76 \times 10^6$	$1.4 \times 10^4$	0.20	1.08	0.86	$4.14 \times 10^{-6}$	$3.84 \times 10^4$	164	1.1	$3.88 \times 10^{-1}$
49	$4.08 \times 10^6$	$1.5 \times 10^4$	0.22	1.11	0.87	$7.60 \times 10^{-6}$	$2.09 \times 10^4$	188	1.4	$2.42 \times 10^{-1}$
45	$4.57 \times 10^6$	$1.4 \times 10^4$	0.27	1.21	0.88	$1.39 \times 10^{-5}$	$1.14 \times 10^4$	184	1.4	$1.41 \times 10^{-1}$
41	$4.60 \times 10^6$	$1.3 \times 10^4$	0.26	1.20	0.89	$3.03 \times 10^{-5}$	$5.25 \times 10^3$	166	1.7	$7.69 \times 10^{-2}$
37	$4.62 \times 10^6$	$1.9 \times 10^4$	0.25	1.14	0.86	$8.66 \times 10^{-5}$	$1.84 \times 10^3$	158	2.1	$3.70 \times 10^{-2}$
33	$4.62 \times 10^6$	$1.9 \times 10^4$	0.23	1.00	0.77	$4.10 \times 10^{-4}$	$3.88 \times 10^2$	162	2.3	$1.41 \times 10^{-2}$
<b>K<sub>0.15</sub>Rb<sub>0.15</sub>MoO<sub>3</sub></b>										
77	$8.80 \times 10^5$		0.25	0.75	0.56	$5.70 \times 10^{-8}$	$2.79 \times 10^6$	92	0.9	3.23
73	$1.05 \times 10^6$		0.29	0.85	0.60	$7.20 \times 10^{-8}$	$2.21 \times 10^6$	96	0.8	2.35
69	$1.24 \times 10^6$		0.30	0.92	0.64	$1.04 \times 10^{-7}$	$1.53 \times 10^6$	108	1.0	1.67
65	$1.47 \times 10^6$		0.31	1.00	0.69	$1.51 \times 10^{-7}$	$1.05 \times 10^6$	146	1.1	1.20
61	$1.86 \times 10^6$		0.34	1.12	0.74	$2.86 \times 10^{-7}$	$5.56 \times 10^5$	130	1.0	$6.90 \times 10^{-1}$
57	$2.13 \times 10^6$	$1.0 \times 10^4$	0.33	1.20	0.80	$5.00 \times 10^{-7}$	$3.18 \times 10^5$	108	1.0	$4.44 \times 10^{-1}$
53	$2.33 \times 10^6$	$2.0 \times 10^4$	0.30	1.15	0.81	$1.15 \times 10^{-6}$	$1.38 \times 10^5$	176	1.0	$2.76 \times 10^{-1}$
49	$2.48 \times 10^6$	$2.0 \times 10^4$	0.30	1.17	0.82	$2.68 \times 10^{-6}$	$5.94 \times 10^4$	180	1.3	$1.67 \times 10^{-1}$
45	$2.34 \times 10^6$	$2.5 \times 10^4$	0.30	1.17	0.82	$5.91 \times 10^{-6}$	$2.69 \times 10^4$	182	1.4	$1.05 \times 10^{-1}$
41	$2.05 \times 10^6$	$2.5 \times 10^4$	0.26	1.00	0.74	$1.76 \times 10^{-6}$	$9.04 \times 10^3$	158	2.0	$6.47 \times 10^{-2}$
37	$1.87 \times 10^6$	$2.0 \times 10^4$	0.24	0.86	0.65	$6.68 \times 10^{-5}$	$2.38 \times 10^3$	168	2.5	$3.55 \times 10^{-2}$
33	$1.74 \times 10^6$	$1.5 \times 10^4$	0.28	0.76	0.55	$4.00 \times 10^{-4}$	$3.98 \times 10^2$	168	5.4	$1.60 \times 10^{-2}$
<b>K<sub>0.3</sub>Mo<sub>0.996</sub>W<sub>0.004</sub>O<sub>3</sub></b>										
69	$5.52 \times 10^4$		0.33	1.17	0.76	$9.90 \times 10^{-9}$	$1.61 \times 10^7$	70	1.9	2.86
65	$5.57 \times 10^4$		0.34	1.16	0.77	$9.90 \times 10^{-8}$	$1.25 \times 10^7$	80	1.6	2.16
61	$5.61 \times 10^4$		0.34	1.08	0.71	$2.11 \times 10^{-8}$	$7.54 \times 10^6$	82	1.8	1.58
57	$5.61 \times 10^4$		0.34	1.02	0.67	$3.52 \times 10^{-8}$	$4.52 \times 10^6$	82	1.5	1.12
53	$5.66 \times 10^4$		0.34	0.91	0.60	$7.22 \times 10^{-8}$	$2.20 \times 10^6$	88	1.8	$7.70 \times 10^{-1}$
49	$5.71 \times 10^4$	$1.5 \times 10^3$	0.34	0.94	0.62	$1.37 \times 10^{-7}$	$1.16 \times 10^6$	102	1.3	$4.93 \times 10^{-1}$
45	$5.71 \times 10^4$	$3.0 \times 10^3$	0.34	0.96	0.63	$2.81 \times 10^{-7}$	$5.66 \times 10^5$	124	2.0	$2.97 \times 10^{-1}$
41	$5.66 \times 10^4$	$3.0 \times 10^3$	0.37	0.93	0.59	$6.65 \times 10^{-7}$	$2.39 \times 10^5$	112	1.1	$1.69 \times 10^{-1}$
37	$5.52 \times 10^4$	$2.5 \times 10^3$	0.40	0.83	0.50	$2.05 \times 10^{-6}$	$7.76 \times 10^4$	128	2.9	$9.12 \times 10^{-2}$
33	$5.76 \times 10^4$	$2.0 \times 10^3$	0.45	0.77	0.42	$9.80 \times 10^{-6}$	$1.62 \times 10^4$	124	2.9	$4.26 \times 10^{-2}$
<b>K<sub>0.3</sub>Mo<sub>0.99</sub>W<sub>0.01</sub>O<sub>3</sub></b>										
49	$8.37 \times 10^3$		0.42	1.1	0.46	$6.15 \times 10^{-9}$	$2.59 \times 10^7$	68	2.6	$7.18 \times 10^{-1}$
45	$8.71 \times 10^3$		0.47	0.90	0.48	$2.20 \times 10^{-8}$	$6.92 \times 10^6$	68	2.6	$4.34 \times 10^{-1}$
41	$8.62 \times 10^3$	$8.5 \times 10^2$	0.47	0.85	0.45	$6.70 \times 10^{-8}$	$2.38 \times 10^6$	78	3.3	$2.48 \times 10^{-1}$
37	$8.62 \times 10^3$	$1.0 \times 10^3$	0.50	0.88	0.44	$1.55 \times 10^{-7}$	$1.03 \times 10^6$	108	2.2	$1.36 \times 10^{-1}$
33	$8.62 \times 10^3$	$1.0 \times 10^3$	0.55	0.97	0.44	$3.00 \times 10^{-7}$	$5.31 \times 10^5$	114	2.3	$6.69 \times 10^{-2}$
29	$8.62 \times 10^3$	$1.0 \times 10^3$	0.60	1.05	0.42	$6.25 \times 10^{-7}$	$2.55 \times 10^5$	126	3.3	$3.24 \times 10^{-2}$
25	$8.12 \times 10^3$	$1.0 \times 10^3$	0.65	1.25	0.44	$7.30 \times 10^{-7}$	$2.18 \times 10^5$	110	3.3	$1.37 \times 10^{-2}$

$${}^a R = \sum_{\omega} [ |\epsilon'_{\text{obs}}(\omega) - \epsilon'_{\text{calc}}(\omega)| + |\epsilon''_{\text{obs}}(\omega) - \epsilon''_{\text{calc}}(\omega)| ] / \sum_{\omega} [ \epsilon'_{\text{obs}}(\omega) + \epsilon''_{\text{obs}}(\omega) ].$$

<sup>b</sup> $\sigma_0$  is a measured value and is not varied in fits to dielectric function.

doped K<sub>0.3</sub>MoO<sub>3</sub> are summarized in Fig. 5, where mean relaxation time is plotted as a function of reciprocal temperature for all compositions. For a particular tempera-

ture the impurities dramatically decrease the mean relaxation time of the CDW, with the tungsten substitutions having the largest effect. At 65 K, for instance, the mean

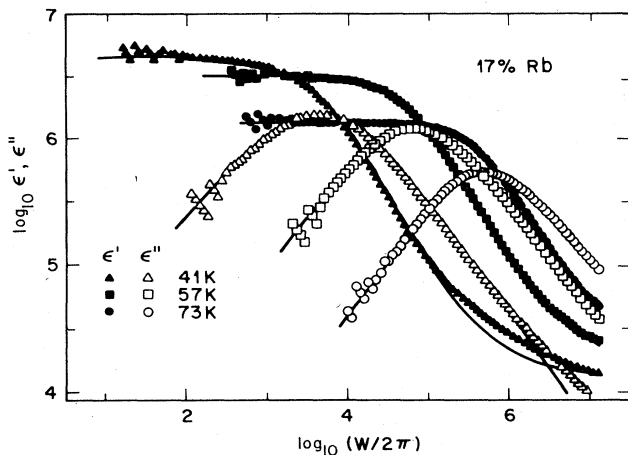


FIG. 1. Real and imaginary parts of the dielectric constant at three representative temperatures as a function of frequency for  $K_{0.25}Rb_{0.05}MoO_3$ . Solid lines are from the fits of Eq. (1) to the data.

relaxation times of the CDW are approximately  $1.6 \times 10^{-5}$  sec for the undoped bronze,  $9.3 \times 10^{-7}$  sec for 17 at. % Rb substituted,  $1.5 \times 10^{-7}$  sec for 50 at. % Rb substituted, and  $1.3 \times 10^{-8}$  sec for 0.4 at. % tungsten substituted bronzes, with the relaxation time too short to measure by our technique at this temperature for the 1 at. % tungsten substitution. Thus a difference of 3 orders of magnitude is observed in  $\tau_0$ , while the threshold field for nonlinear conductivity has been changed by 1 order of magnitude or less. The present data have been taken over a significantly wider temperature range than those of the previous study and generally show a more complex temperature dependence of  $\tau_0$  than the simple linear  $\log_{10}\tau_0$  versus  $1/T$  seen in  $K_{0.3}MoO_3$ . For the Rb substituted samples, for instance, plots of  $\log_{10}\tau_0$  against  $1/T$  display a change in slope within the range of measurement, which is most pronounced in the 17 at. % Rb substitution. We do not know whether this change in slope occurs at low

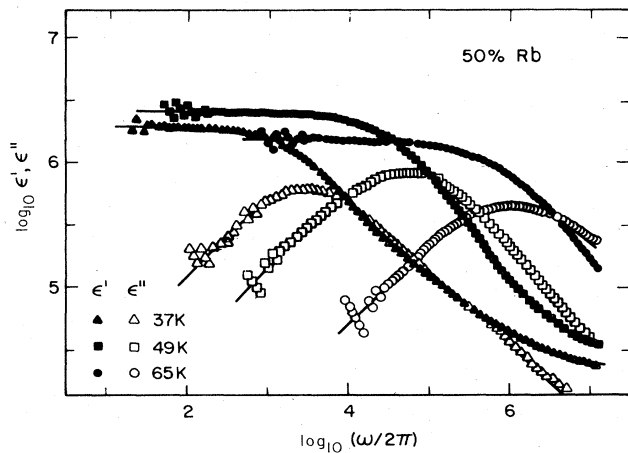


FIG. 2. Real and imaginary parts of the dielectric constant at three representative temperatures as a function of frequency for  $K_{0.15}Rb_{0.15}MoO_3$ . Solid lines are from the fits of Eq. (1) to the data.

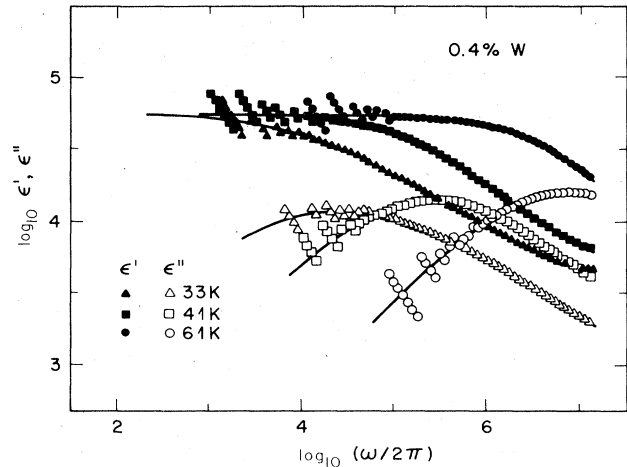


FIG. 3. Real and imaginary parts of the dielectric constant at three representative temperatures as a function of frequency for  $K_{0.30}Mo_{0.996}W_{0.004}O_3$ . Solid lines are from the fits of Eq. (1) to the data.

temperatures in the undoped bronze. The data for the 0.4 at. % tungsten substitution follow reasonable straight-line behavior over the whole temperature range studied, whereas the 1 at. % tungsten substituted data fall on a continuously curved line in the temperature-time range accessible by our technique. The activation energies for the relaxation times are approximately 829 K for the undoped bronze, 626 K (high temperature) and 371 K (low temperature) for the 17 at. % Rb substituted material, 556 K (high temperature) and 467 (low temperature) for the

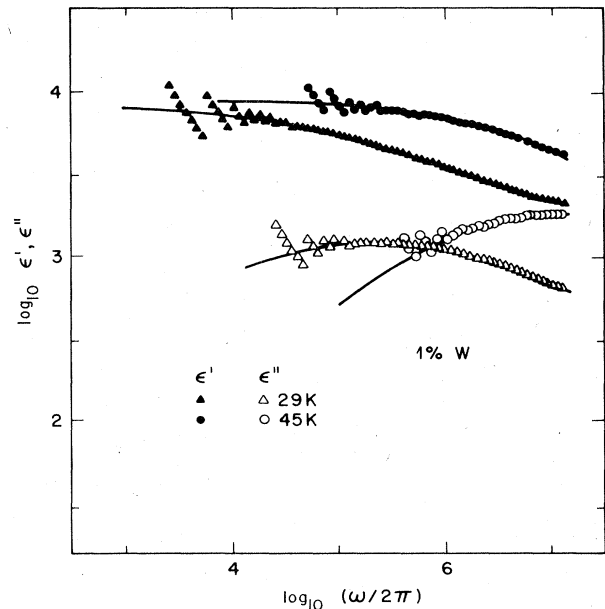


FIG. 4. Real and imaginary parts of the dielectric constant at three representative temperatures as a function of frequency for  $K_{0.30}Mo_{0.99}W_{0.01}O_3$ . Solid lines are from the fits of Eq. (1) to the data.

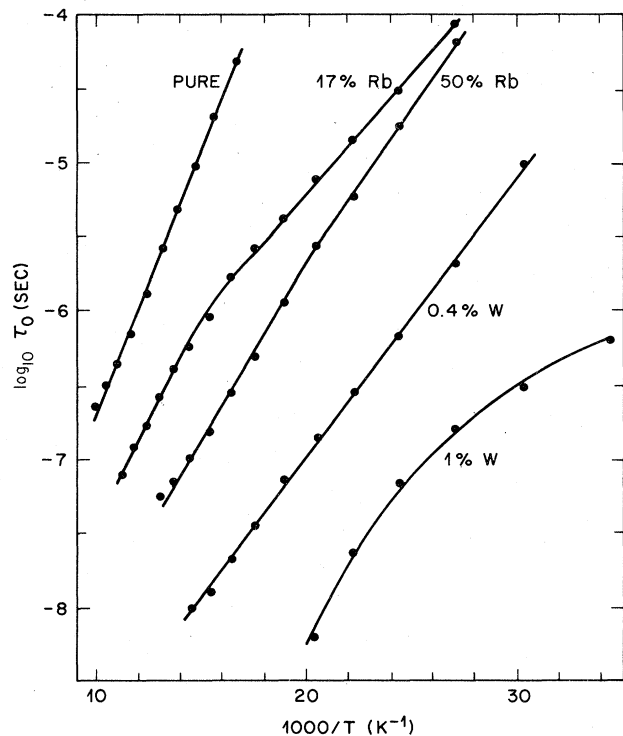


FIG. 5. Temperature dependence of the mean relaxation time  $\tau_0$  for pure and impurity doped bronzes: Pure,  $K_{0.3}MoO_3$ ; 17 at. % Rb,  $K_{0.25}Rb_{0.05}MoO_3$ ; 50 at. % Rb,  $K_{0.15}Rb_{0.15}MoO_3$ ; 0.4 at. % W,  $K_{0.30}Mo_{0.996}W_{0.004}O_3$ ; 1 at. % W,  $K_{0.30}Mo_{0.99}W_{0.01}O_3$ .

50 at. % Rb substituted material, 432 K for the 0.4 at. % tungsten substituted material, and varying between approximately 590 and 200 K for the 1 at. % tungsten substituted material. The 50 at. % Rb substituted bronze crystal shows evidence for the beginning of a change in slope to a lower value at the highest temperatures measured.

The static dielectric constants  $\epsilon_0$  are also dramatically effected by impurities. The trends in the observed static dielectric constants (Table II) are summarized in Fig. 6, along with a comparison to our results for the undoped bronze. Again selecting a temperature of 65 K for comparison purposes, we find static dielectric constants of approximately  $2.2 \times 10^7$  for the undoped bronze,  $2.1 \times 10^6$  for the 17 at. % Rb substituted material,  $1.5 \times 10^6$  for the 50 at. % Rb substituted material,  $5.6 \times 10^4$  for the 0.4 at. % W substituted material, and  $8.6 \times 10^3$  (extrapolated) for the 1 at. % w substituted material. As observed for the relaxation times, the static dielectric constants show a variation of approximately 3 orders of magnitude over the range of impurity concentrations studied here. The temperature variation of the static dielectric constants is significantly different from that of the relaxation times. For both tungsten-doped samples,  $\epsilon_0$  is independent of temperature, whereas for the 17 at. % rubidium content sample,  $\epsilon_0$  saturates for temperatures below approximately 45 K. We do not know whether  $\epsilon_0$  saturates for the undoped bronze at low temperatures. For the 50 at. % Rb sample,

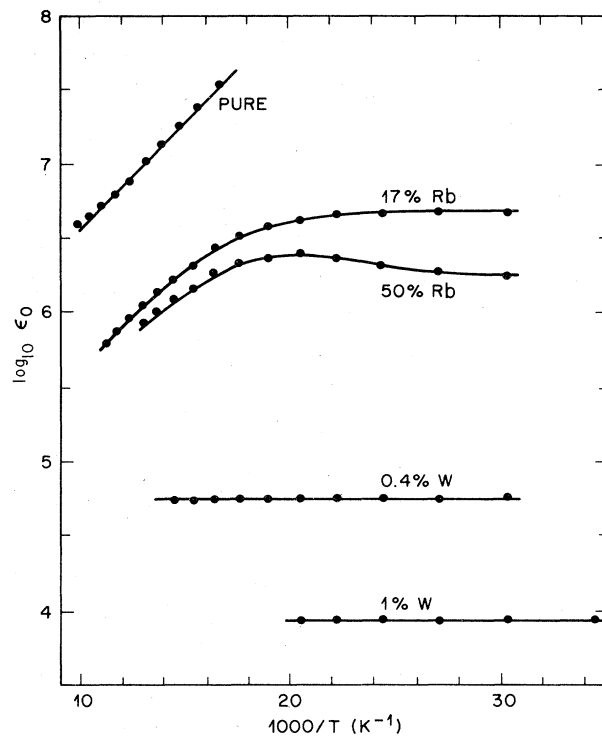


FIG. 6. Temperature dependence of the static dielectric constant,  $\epsilon_0$ , for pure and impurity doped bronzes: Pure,  $K_{0.30}MoO_3$ ; 17 at. % Rb,  $K_{0.25}Rb_{0.05}MoO_3$ ; 50 at. % Rb,  $K_{0.15}Rb_{0.15}MoO_3$ ; 0.4 at. % W,  $K_{0.30}Mo_{0.996}W_{0.004}O_3$ ; 1 at. % W,  $K_{0.30}Mo_{0.99}W_{0.01}O_3$ .

the static dielectric constant displays an initial increase and then a decrease to a value which appears to be saturating at low temperatures. In the higher-temperature region the activation energies for  $\epsilon_0$  are 307 K for the 17 at. % Rb material and 212 K for the 50 at. % Rb material, considerably smaller than the 334 K observed for the undoped bronze.

Due to the unusual behavior of  $\epsilon_0$  with temperature in the 50 at. % Rb substituted material, we performed a measurement of the temperature dependence of the threshold field for nonlinear conductivity ( $E_T$ ) in the same temperature range. The results are presented in Fig. 7. We find  $E_T$  to display a minimum in the same temperature range where  $\epsilon_0$  displays a maximum; however, the product of  $\epsilon_0 E_T$  is not constant and appears to be diverging at low temperatures where  $\epsilon_0$  is saturating and  $E_T$  is increasing rapidly. For temperatures below 35 K the response of the sample measured in the dc  $I$ - $V$  traces is dominated by metastable states of the CDW, as the response is dependent on the sweep rate of the driving current. We expect the occurrence of long-time relaxations which would effect dc  $I$ - $V$  traces even below  $E_T$  at low temperatures as the characteristic mean relaxation time is  $4 \times 10^{-4}$  sec ( $\omega_0/2\pi \approx 400$  Hz) at 33 K with a broad distribution of times.

The impurities also have a significant effect on the distribution of relaxation times. The distribution function for the 17 at. % Rb substituted material displays the same

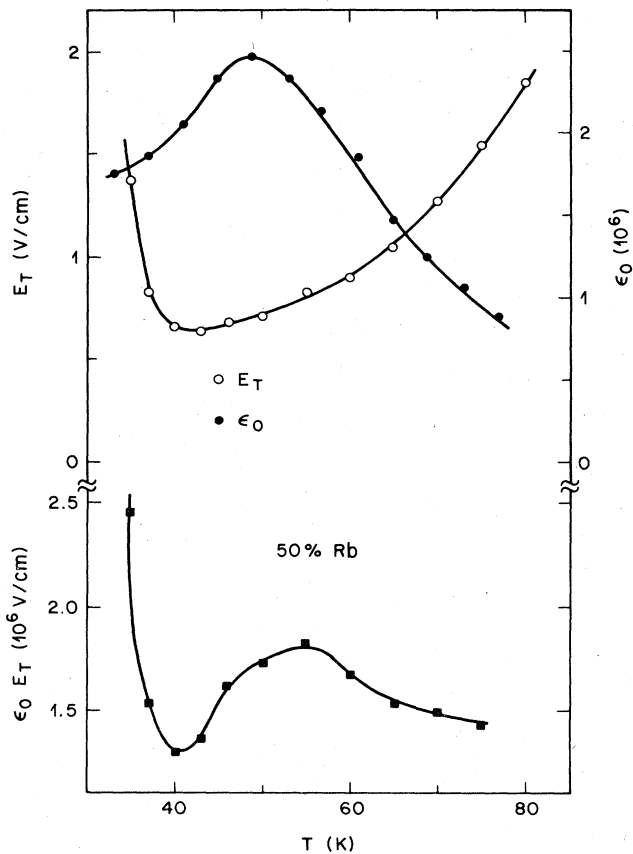


FIG. 7. Temperature dependence of the threshold field for nonlinear conduction,  $E_T$ , static dielectric constant  $\epsilon_0$ , and their product,  $\epsilon_0 E_T$ , for  $K_{0.15}Rb_{0.15}MoO_3$ .

general characteristics as the undoped material:  $\alpha$  is small (narrow distribution) at high temperatures but increases, thus indicating an increasingly broadening distribution of times at low temperatures. The parameters  $[\beta(1-\alpha)]$  describing the distribution of relaxations for  $\tau < \tau_0$  are essentially independent of temperature at high temperatures, as is observed in the undoped material, but then change significantly at lower temperatures (below approximately 50 K). We do not know whether a similar change occurs in the undoped bronzes. For the high-impurity materials the width of the distribution of relaxations is not as strongly temperature dependent, but also broadens with decreasing temperature. The distribution of relaxation times becomes broader with increasing impurity concentration and is very broad for the 1 at. % tungsten substituted material.

In contrast to our earlier study on  $K_{0.3}MoO_3$ , in the doped materials we were able to follow the dielectric response to frequencies where the high-frequency dielectric constant  $\epsilon_{HF}$  [Eq. (2)] became significant in the fits. The values obtained for  $\epsilon_{HF}$  are included in Table II. While  $\epsilon_{HF}$  values are known to be significantly less accurate than  $\epsilon_0$ , values they also, where determined, show some temperature dependence in the Rb substituted materials and little (within the sensitivity of the fit) tempera-

ture dependence in the tungsten substituted materials. The values of  $\epsilon_{HF}$  are different for the different materials, showing a decrease in magnitude for higher dopant levels. The decrease is significantly less pronounced than that observed for the static dielectric constants  $\epsilon_0$ . Thus the high-frequency real dielectric constant  $\epsilon_{HF}$  is likely to be an "intermediate"-frequency value: it occurs at frequencies much larger than  $\omega_0/2\pi$  where the low-frequency relaxation cannot respond to the applied field and represents the "static" dielectric constant for a relaxation probably related to CDW dynamics at higher frequencies. Reported  $\sigma(\omega)$  data for pure bronze crystals do not clearly indicate the presence of this relaxation at frequencies lower than 500 MHz,<sup>17,18</sup> and optical reflectivity measurements suggest that it might occur in the infrared.<sup>19</sup> Finally, we note deviations in the observed dielectric response from Eq. (2) at low temperatures and high frequencies (Fig. 1). The nature of the deviation is best seen in reference to  $\epsilon''(\omega)$ , which changes slope [and thus has a different  $\beta(1-\alpha)$ ] to a smaller power at high frequency. A power law of  $\omega^{-1/2}$  has been observed in the pure bronze for  $\omega \gg \omega_0$  at low temperatures.<sup>17,18</sup>

We present in Fig. 8 the temperature dependence of the dc resistivity for the various substituted materials, in comparison to that of the undoped bronze over the temperature range of the dielectric constant measurements. In agreement with previous measurements,<sup>9,11</sup> we find the dc resistivity at low temperatures to be significantly decreased for the tungsten substituted materials.

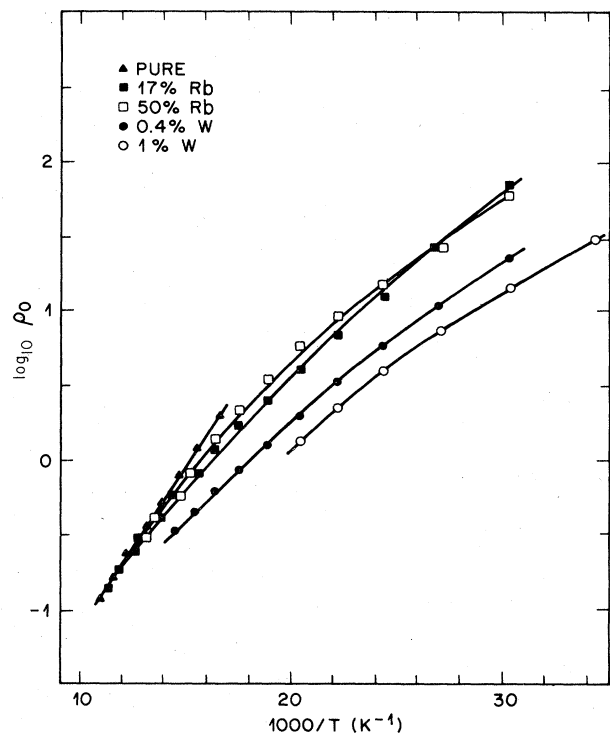


FIG. 8. Temperature dependence of the dc resistivity for pure and impurity doped bronzes: Pure,  $K_{0.30}MoO_3$ ; 17 at. % Rb,  $K_{0.25}Rb_{0.05}MoO_3$ ; 50 at. % Rb,  $K_{0.15}Rb_{0.15}MoO_3$ ; 0.4 at. % W,  $K_{0.30}Mo_{0.996}W_{0.004}O_3$ ; 1 at. % W,  $K_{0.30}Mo_{0.99}W_{0.01}O_3$ .

#### IV. DISCUSSION AND CONCLUSIONS

The characteristics of the dielectric response of the CDW in  $K_{0.3}MoO_3$  are dramatically affected by the introduction of impurities. The dielectric response is more strongly influenced by impurities on the molybdenum sublattice than on the potassium sublattice, in agreement with the measurements of other characteristics. The impurities affect the mean relaxation time of the CDW ( $\tau_0$ ), the breadth and shape of the distribution of times ( $\alpha, \beta$ ), and the dielectric constants for times much longer ( $\epsilon_0$ ) and much shorter ( $\epsilon_{HF}$ ) than the mean relaxation time.

It is of interest to consider our data within the context of the classical model of the pinning of a CDW by impurities due to Fukuyama, Lee, and Rice.<sup>12</sup> In that model, one considers the pinning of an incommensurate CDW of wave vector  $Q$ , described by an order parameter  $\rho_0 \cos[Q \cdot r + \phi(r)]$ . If the effective pinning by disorder is weak, and the correlation length is long, only the effect of long-wavelength phase fluctuations in the CDW is considered, with the Hamiltonian

$$H = \int d^3r \left\{ \frac{1}{2} \kappa |\nabla \phi|^2 + \sum_i v_i(r - R_i) \rho_0 \cos[Q \cdot r + \phi(r)] - \rho_c E \phi(r) / Q_z \right\}. \quad (4)$$

Here,  $K$  described the elasticity of the CDW and  $v_i$  is the potential of an impurity at position  $R_i$ . The electric field  $E$  is assumed to couple to the full collective charge density  $\rho_c$  of the CDW, and  $Q_z$  is the CDW wave vector in the incommensurate  $z$  direction. Within this picture, the dynamics is assumed to be given by an overdamped equation of motion<sup>13</sup>

$$\lambda \dot{\phi} = -\delta H / \delta \phi. \quad (5)$$

The dimensions in Eq. (4) have been scaled to make the elastic constant  $K$  isotropic. Because the CDW is periodic, it interacts most strongly with the short-range components of the impurity potential. For a short-ranged potential an important parameter is the dimensionless coupling constant  $\delta = \rho_0 \langle v^2 \rangle^{1/2} c^{1/3} / K$ , where  $c$  is the impurity concentration. For  $\delta \ll 1$  (weak pinning) the CDW correlation length ( $L$ ) is given by  $Lc^{1/3} = \delta^{-2/3} \gg 1$ , resulting in a correlation length which is much larger than the impurity spacing. For  $\delta \geq 1$ ,  $L \sim c^{-1/3}$ , which is the strongly pinned case, resulting in a correlation length on the order of the impurity spacing. Present experiments indicate that at least for rubidium-doped samples the weak pinning regime is the correct one. The threshold field for sliding can then be estimated by

$$E_T \simeq Q_z E_p / \rho_c, \quad (6)$$

where  $E_p \sim K/L^2$  is the pinning energy per unit volume.

Rather than dealing with the detailed frequency dependence of  $\epsilon(\omega)$  or detailed behavior of the nonlinear conductivity,<sup>13-15,20</sup> we can determine whether the model successfully estimates the relative magnitudes of various quantities. A straightforward analysis gives  $\epsilon_0 \simeq \rho_c / Q_z E_T$ ,  $\tau_0 \sim \lambda Q_z / \rho_c E_T$ , and a value of the high-field CDW conductivity of  $\sigma_{CDW} \simeq \rho_c^2 / \lambda Q_z^2$ . At 77 K, in an undoped sample of  $K_{0.3}MoO_3$ , we also have a measurement of the "washboard" frequency  $\omega_0(E)$  from the frequency depen-

dence of the conductivity in the presence of a dc electric field.<sup>3</sup> Since  $\omega_0 \simeq \rho_c E / Q \lambda$ , and experimentally<sup>3</sup>  $\omega_0 C E \sigma_{CDW}$  with  $C = 0.08 \text{ MHz cm}^2 \text{ A}^{-1}$ , we can estimate  $\rho_c \simeq 4 \times 10^7 \text{ C m}^{-3}$ , which gives a collective charge density corresponding to roughly one electron per unit supercell. From this and the measured values of the threshold field,  $E_T$ , we estimate  $\tau_0 \sim 10^{-6}$  sec and a value of  $\epsilon_0 \sim 10^8$ . Both of these numbers are consistent with the measured values in pure  $K_{0.3}MoO_3$  at 77 K.

Rb substituted for K is expected to be a weakly pinning impurity, with the model predicting that  $\tau_0$  and  $\epsilon_0$  should decrease with increasing  $E_T$ . For a given temperature, such behavior is observed, as one can see in Figs. 5 and 6 and in Table III. However, the effects of W impurities on the Mo sublattice are much more dramatic in changing  $\epsilon_0$  and  $\tau_0$  cannot be accounted for by the change in the threshold field. It is likely that W impurities are strong-pinning centers and may, in fact, locally perturb the amplitude  $\rho_0$  of the CDW as well as its phase, so the analysis given above in terms of phase fluctuations alone is not appropriate. In this case, the threshold field will be controlled by the creation of dislocation loops in the CDW lattice from the analog of Frank-Read sources, as discussed by Lee and Rice.<sup>12</sup>

The most striking feature of the data is the temperature dependence observed in both  $\epsilon_0$  and  $\tau_0$ , which is particularly strong for the pure and Rb-doped materials. At least in the pure material, this cannot be explained by a strong temperature dependence of  $E_T$ , because the threshold field is decreasing only weakly with temperature. However, in the sample of  $K_{0.15}Rb_{0.15}MoO_3$ , where the temperature dependence of  $\epsilon_0$  is less strong, the quantities  $\epsilon_0$  and  $E_T$  vary roughly inversely as each other between 75 and 40 K (see Fig. 7).

Explaining the activated temperature dependence of  $\epsilon_0$  and  $\tau_0$  by a mechanism of thermal hopping of pinned domains of CDW over local barriers is not satisfactory, as such hopping would be expected to wash out any sharp threshold for nonlinear conduction. The characteristic barrier height for a domain will be of order

$$E_d \simeq (\rho_c E_T / Q_z) L_x L_y L_z,$$

where  $L_\alpha$  is the correlation length in the  $\alpha$  direction. For pure blue bronze at 77 K,  $\rho_c E_T / Q_z \simeq 10^{16} \text{ K/cm}^3$ . Surprisingly, even for an average correlation length of 1  $\mu\text{m}$ , this leads to an average barrier height of only  $10^4 \text{ K}$ . The correlation lengths may in fact be significantly shorter than this,<sup>21</sup> particularly perpendicular to the  $b$  axis. Thus direct thermal effects cannot actually be ruled out. A precursor to thermal depinning of the CDW could be a rounding out in the low-frequency cusp in  $\epsilon'(\omega)$  with increasing temperature. Within our analysis of the data, this would appear as a decreasing value of  $\alpha$  with increasing temperature, behavior which is seen for both the pure and 17 at. % Rb-doped samples. The existence of a sharp threshold in all these materials at high temperatures, however, seems to be good evidence against thermal activation over the large barriers which determine the threshold field and the response  $\epsilon(\omega)$  at frequencies close to  $1/\tau_0$ .

TABLE III. Characteristics of CDW dielectric response in various Potassium Molybdate blue bronzes at 77 K.

Sample	$\epsilon_0$	$\omega_0/2\pi$ (Hz)	$E_T$ (mV/cm)	$\alpha$	$\beta(1-\alpha)$
$K_{0.3}MoO_3$	$3.48 \times 10^6$	$6.34 \times 10^4$	61	0.20	0.81
$K_{0.3}MoO_3^a$	$8.47 \times 10^6$	$7.58 \times 10^4$	113	0.18	0.71
$K_{0.3}MoO_3^b$	$4.31 \times 10^6$	$3.17 \times 10^5$	130	0.26	0.75
$K_{0.25}Rb_{0.05}MoO_3$	$1.12 \times 10^6$	$5.98 \times 10^5$	680	0.08	0.75
$K_{0.15}Rb_{0.15}MoO_3$	$8.80 \times 10^5$	$2.79 \times 10^6$	1640	0.25	0.56

<sup>a</sup>The sample employed in earlier detailed analysis of temperature-dependent dielectric response (Ref. 3).

<sup>b</sup>This sample employed in earlier studies of thermally stimulated depolarization of the CDW (Ref. 28), effect of ac signal level on CDW response (Ref. 4), and inductive ringing in response to applied dc pulse (Ref. 29).

The analysis of Eq. (4) is based on the assumption of an incommensurate CDW pinned by disorder. As  $K_{0.3}MoO_3$  is believed to undergo a lock-in transition to a commensurate phase at about 110 K,<sup>22</sup> we must also consider the effects of pinning to the lattice. Within a Landau theory, commensurability pinning can be included in Eq. (4) by adding a term  $V \cos[p(\phi + (\mathbf{Q} - \mathbf{Q}_c) \cdot \mathbf{r})]$ , where  $p$  ( $=4$ ) is the order of commensurability,  $V$  the strength of the pinning, the  $\mathbf{Q}_c$  the commensurate wave vector.<sup>23</sup> Close to the onset of a second-order transition, the commensurability pinning vanished ( $V\alpha\rho_0^b$ ) and the CDW is uniform with wave vector  $\mathbf{Q}$ . Close to the commensurate-incommensurate transition, the CDW is better described by an array of widely spaced discommensurations,<sup>23</sup> which have a typical thickness  $2\eta = (8\pi/p)(\mathbf{Q} - \mathbf{Q}_c)^{-1} \simeq 60$  Å. The commensurate regions are strongly pinned by the lattice, and will not slide in an electric field. Following this analysis, one estimates a threshold field for commensurate sliding of  $(KQ_c/\rho_c)\eta^{-2} \simeq 1$  kV/cm. This implies a high-frequency dielectric constant  $\epsilon_{HF}$  of order  $10^4$  and a loss peak at a frequency  $\sim 10^{10}$  Mz or higher. Such a mode may have been observed in the far infrared.<sup>18</sup>

Within this picture, the CDW current is carried by discommensurations<sup>24</sup> at low temperatures. The discommensurations themselves will be pinned by impurities<sup>25</sup> and one does not expect an abrupt change in the threshold field between the high-temperature regime of an incommensurate CDW and the low-temperature region where transport is assumed to be via discommensurations. However, the density of discommensurations at low temperatures should be very low, and the magnitude of the current should be small. While it is true that the magnitude of the nonlinear conductivity drops sharply at low temperatures,<sup>26</sup> the dielectric constant  $\epsilon_0$  grows in an activated fashion, as we have remarked above. The opposite behavior of  $\epsilon_0$  and  $\sigma_{CDW}$  is very hard to reconcile, whatever model one uses.

A separate complication in all these materials is that they become insulating at low temperatures. The temperature dependence of the dc resistivity is shown in Fig. 8. The electronic band structure is sufficiently anisotropic such that the CDW introduces a gap over the whole of the Fermi surface; from the slopes in Fig. 8 we estimate the CDW gap  $2\Delta \simeq 1000$  K. At low temperatures when the carrier density is small, one may expect Coulombic in-

teractions of the CDW with itself will become important, which will lead to an increase in the effective elastic constant  $K$  of Eq. (4). We do not expect that screening will affect the interaction with impurities, because this is predominantly short range.

An approximate screening length can be calculated from expressions for dependence of screening length on temperature and carrier density and the dependence of carrier density on temperature and bandgap.<sup>27</sup> We take the electron and hole effective masses to be unity and find  $l_s(\text{Å}) \simeq 10T^{-1/4} e^{E_g/4k_B T}$  where  $l_s$  is the screening length in angstroms and  $E_g$  is the gap. From estimates of the observed variations of  $\ln\rho_0$  versus  $1/T$  at low temperatures, the screening lengths (which are roughly the same for all compositions) are approximately  $10^6$  Å at 10 K,  $10^4$  Å at 15 K,  $10^3$  Å at 25 K,  $10^2$  Å at 40 K, and less than 25 Å for temperatures greater than 60 K. The change in screening length from  $10^4$  to  $10^2$  Å between 15 and 40 K suggests that this temperature interval is a likely one in which changes in the dynamics of the CDW might occur as the correlation length will be constant (and much smaller than the screening length) at very low temperatures, determined by the *unscreened* elastic stiffness of the CDW. As the temperature is raised,  $l_s$  will approach the correlation length  $L$  and the long-wavelength fluctuations of the CDW will be screened. Over some region of temperature,  $L$  should then decrease, following  $l_s$ , until  $L$  saturates at a high-temperature value corresponding to the *screened* elastic CDW stiffness. The dominant effects will presumably be on the shorter transverse correlation length, especially if the charge transport is via discommensurations. This will lead to an increase in  $\epsilon_0$  and  $\tau_0$  with decreasing temperature in the crossover region, and a saturation at very low temperatures. The screening effect should be more important for weakly pinned samples where the disorder is relatively weak; in the case of strong pinning the correlation length is determined only by disorder, and the elastic stiffness of the CDW is not relevant. This crossover might explain the behavior of  $\epsilon_0$  and  $\tau_0$  shown in Figs. 6 and 7. However, the temperature region where activated behavior is seen is rather high ( $T > 50$  K), to be explained by the values of  $l_s$  we estimated above. Moreover, this picture would be expected to lead to the same temperature dependence for  $\epsilon_0$  and  $\tau_0$  as well as (decreasing) activated behavior for  $E_T$ , which is not in accord with our observations. Because the electronic band

structure is highly anisotropic, the screening length  $l_s$  calculated above is strictly valid only for screening parallel to the  $b$  axis. The screening length perpendicular to the chains could be determined by the transverse overlap of the wave functions from different chains, which could lead to a much longer  $l_s$  in the transverse directions, and thereby produce activated behavior at higher temperatures.

It is clear that the classical picture of the pinning of a CDW by impurities does produce a qualitatively accurate description of the data, but does not give a good quantitative explanation of the temperature dependence of the measured parameters. We have run through several plausible explanations for the variation of  $\epsilon_0$ ,  $\tau_0$ , and  $E_T$  from a microscopic point of view, and find that while the effect of disorder is as expected, the temperature dependence is not easy to account for. The classical model does describe accurately a large number of phenomena observed in sliding CDW systems, for example metastability,<sup>28</sup> the cusp-like behavior in  $\epsilon(\omega)$  at low frequencies,<sup>3</sup> a "ringing" response to a sudden change in driving voltage,<sup>29</sup> the dependence of  $\epsilon(\omega)$  on dc driving field,<sup>3,20</sup> and the non-

linear  $I$ - $V$  characteristic.<sup>13,14,20</sup> What is missing is a microscopic derivation of the various parameters. We feel that thermal effects, the commensurate-incommensurate transition, and the change in screening at low temperatures will all be important in determining the behavior. We note that while all the sliding CDW systems show roughly the same qualitative behavior, the detailed temperature dependence is very different in other materials.<sup>30</sup>

Finally, the unusual temperature dependence of  $\epsilon_0$  and  $E_T$  in  $\text{K}_{0.15}\text{Rb}_{0.15}\text{MoO}_3$  suggests that some additional process is occurring at low temperatures in this sample. The simple 1:1 ratio of K to Rb suggests that there may be some short-range order among the alkali metals which has an effect on CDW behavior at low temperatures. We are currently investigating the x-ray scattering from samples of this composition to test this hypothesis.

#### ACKNOWLEDGMENTS

We acknowledge helpful discussions with D. S. Fisher and the technical assistance of S. E. Spengler.

- 
- <sup>1</sup>J. Dumas, C. Schlenker, J. Marcus, and R. Buder, *Phys. Rev. Lett.* **50**, 757 (1983).
- <sup>2</sup>See, for instance, *Charge Density Waves in Solids*, Vol. 27 of *Lecture Notes in Physics*, edited by Gy. Hutiray and J. Sólyom (Springer, Berlin, 1985).
- <sup>3</sup>R. J. Cava, R. M. Fleming, P. Littlewood, E. A. Rietman, L. F. Schneemeyer, and R. G. Dunn, *Phys. Rev. B* **30**, 3228 (1984).
- <sup>4</sup>R. J. Cava, R. M. Fleming, R. G. Dunn, E. A. Rietman and L. F. Schneemeyer, *Phys. Rev. B* **30**, 7290 (1984).
- <sup>5</sup>A. Zettl and G. Grüner, *Phys. Rev. B* **29**, 755 (1983).
- <sup>6</sup>G. Grüner, A. Zawadowski, and P. M. Chaikin, *Phys. Rev. Lett.* **46**, 511 (1981).
- <sup>7</sup>P. Debye, *Polar Molecules* (Chemical Catalog Co., New York, 1929).
- <sup>8</sup>S. Havriliak and S. Negami, *J. Polym. Sci. C* **14**, 99 (1966).
- <sup>9</sup>L. F. Schneemeyer, F. J. DiSalvo, S. E. Spengler, and J. V. Waszczak, *Phys. Rev. B* **30**, 4297 (1984).
- <sup>10</sup>L. F. Schneemeyer, R. M. Fleming, and S. E. Spengler *Solid State Commun.* **53**, 505 (1984).
- <sup>11</sup>L. F. Schneemeyer, S. E. Spengler, F. J. DiSalvo, and J. V. Waszczak, *Mol. Cryst. Liq. Cryst.* (to be published).
- <sup>12</sup>H. Fukuyama and P. A. Lee, *Phys. Rev. B* **17**, 535 (1978); P. A. Lee and T. M. Rice, *ibid.* **19**, 3970 (1979).
- <sup>13</sup>L. Sneddon, M. C. Cross, and D. S. Fisher, *Phys. Rev. Lett.* **49**, 292 (1982).
- <sup>14</sup>D. S. Fisher, *Phys. Rev. Lett.* **50**, 1486 (1983); and *Phys. Rev. B* **31**, 1396 (1985).
- <sup>15</sup>P. B. Littlewood, in *Charge Density Waves in Solids*, Ref. 2, p. 369.
- <sup>16</sup>A. Wold, W. Kunnmann, R. J. Arnett, and A. Ferretti, *Inorg. Chem.* **3**, 545 (1964).
- <sup>17</sup>D. Reager and G. Mozurkewich (unpublished).
- <sup>18</sup>See R. P. Hall, M. Sherwin, and A. Zettl in *Charge Density Waves in Solids*, Ref. 2, p. 314.
- <sup>19</sup>See G. Travaglini and P. Wachter in *Charge Density Waves in Solids*, Ref. 2, p. 115.
- <sup>20</sup>L. Sneddon, *Phys. Rev. Lett.* **52**, 65 (1984); *Phys. Rev. B* **29**, 719 and 725 (1984).
- <sup>21</sup>R. M. Fleming, R. G. Dunn, and L. F. Schneemeyer, *Phys. Rev. B* **31**, 4099 (1985).
- <sup>22</sup>R. M. Fleming, L. F. Schneemeyer, and D. E. Moncton, *Phys. Rev. B* **31**, 899 (1985).
- <sup>23</sup>W. L. McMillan, *Phys. Rev. B* **14**, 1496 (1976).
- <sup>24</sup>T. M. Rice, in *Charge Density Waves in Solids*, Ref. 2, p. 1.
- <sup>25</sup>T. M. Rice, S. Whitehouse, and P. B. Littlewood, *Phys. Rev. B* **24**, 2751 (1981).
- <sup>26</sup>R. M. Fleming, R. J. Cava, E. A. Rietman, R. G. Dunn, and L. F. Schneemeyer (unpublished).
- <sup>27</sup>See, for instance, J. M. Ziman, *Theory of Solids* (Cambridge University Press, London, 1972), pp. 142 and 151.
- <sup>28</sup>R. J. Cava, R. M. Fleming, E. A. Rietman, R. G. Dunn, and L. F. Schneemeyer, *Phys. Rev. Lett.* **53**, 1677 (1984).
- <sup>29</sup>R. M. Fleming, L. F. Schneemeyer, and R. J. Cava, *Phys. Rev. B* **31**, 1181 (1985); S. N. Coppersmith and P. B. Littlewood, *ibid.* **31**, 4049 (1985).
- <sup>30</sup>R. J. Cava, R. M. Fleming, R. G. Dunn, and E. A. Rietman (unpublished).